Journal of the Korean Ceramic Society
Vol. 52, No. 6, pp. 441~448, 2015.

http://dx.doi.org/10.4191/kcers.2015.52.6.441

High-Temperature Fracture Strength of a CVD-SiC Coating Layer for TRISO Nuclear Fuel Particles by a Micro-Tensile Test

Hyun Min Lee, Kwi-Il Park, Ji-Yeon Park*, Weon-Ju Kim*, and Do Kyung Kim†

Department of Materials Science and Engineering,
Korea Advanced Institute of Science and Technology (KAIST), Daejeon 34141, Korea
**Nuclear Materials Research Division, Korea Atomic Energy Research Institute (KAERI), Daejeon 34057, Korea*

(Received September 1, 2015; Revised October 22, 2015; Accepted October 27, 2015)

ABSTRACT

Silicon carbide (SiC) coatings for tri-isotropic (TRISO) nuclear fuel particles were fabricated using a chemical vapor deposition (CVD) process onto graphite. A micro-tensile-testing system was developed for the mechanical characterization of SiC coatings at high temperatures. The fracture strength of the SiC coatings was characterized by the developed micro-tensile test in the range of 25°C to 1000°C. Two types of CVD-SiC films were prepared for the micro-tensile test. SiC-A exhibited a large grain size (0.4 ~ 0.6 m) and the [111] preferred orientation, while SiC-B had a small grain size (0.2 ~ 0.3 mm) and the [220] preferred orientation. Free silicon (Si) was co-deposited onto SiC-B, and stacking faults also existed in the SiC-B structure. The fracture strengths of the CVD-SiC coatings, as measured by the high-temperature micro-tensile test, decreased with the testing temperature. The high-temperature fracture strengths of CVD-SiC coatings were related to the microstructure and defects of the CVD-SiC coatings.

Key words : SiC coating layer, TRISO, Micro-tensile-test, High temperature fracture strength, Weibull statistics

I. Introduction

Silicon carbide (SiC) film and fiber-reinforced SiC composites have attracted considerable research attention due to their unique physical properties, such as their low electrical conductivity, low thermal decay, low level of tritium permeability, good resistance to neutron irradiation, and high mechanical properties.[1-4] Thus, SiC is one of the most interesting materials in several fields, ranging from nuclear power plants for fusion blankets to functional materials. Recently, SiC-MEMS sensors were used in harsh-environment applications.[5,6] Chemically deposited SiC coatings have gained interest for utilization as a pressure vessel in TRISO (TRistructural ISOtropic) nuclear fuel particles to develop a very-high-temperature gas-cooled reactor (VHTR). The TRISO coating system has become the most common technique used for the fabrication of fuel for VHTRs. It contains internal gas pressure which is generated during the fission of the fuel kernel material, acting as a diffusion barrier to metallic fission products. The coating layer adjacent to the fuel kernel is a low-density buffer layer with approximately 50% porosity. This layer absorbs fission-product recoils from the kernel, provides a reservoir for fission product gases, and accommodates kernel-swelling limiting forces transmitted to the outer coatings. The next layer is a high-density, isotropic inner PyC (pyrolytic carbon) layer that protects the kernel from reactions with chlorine present during the deposition of the SiC layer, provides structural support for the SiC layer, and protects the SiC from fission products and carbon monoxide during operation. The outermost layer is another high-density, isotropic outer PyC layer that protects the SiC during the remainder of the fabrication process and imparts structural stability to the particles during irradiation.[7,8] The significance of SiC coatings is that they maintain the strength of the TRISO particles from the internal pressure exerted by gas evolution from the inner sides of the particles.[9-13]

From the point of view on safety of the fusion structures, it is necessary to study their facture strength and the behavior of materials precisely with the same dimensions and fabrication processes of TRISO nuclear fuel particles. In the literature, there are several reports on the fracture strength of the SiC coatings at room temperature,[2,14] However studies at higher temperatures, which are the actual working temperature of TRISO nuclear fuel particles in reactors, are negligibly few. Therefore, a detailed investigation of the fracture strength at higher temperatures is necessary for the SiC coatings used in TRISO nuclear fuel particles operating in harsh environments.

In the present case, micro-tensile system was newly developed for the mechanical characterization of SiC thin films at elevated temperatures. Two types of SiC coatings were prepared for the micro-tensile test, which were fabricated by a chemical vapor deposition process. Scanning

†Corresponding author : Do Kyung Kim
E-mail : dkkim@kaist.ac.kr
Tel : +82-42-350-4118 Fax : +82-42-350-3310

electron microscopy, X-ray diffractometry, transmission electron microscopy, and Raman spectroscopy were used to characterize the SiC coatings. We fabricated SiC micro-tensile specimens based on our tensile testing system and conducted the micro-tensile test. The fracture strength of the SiC coatings as measured by the micro-tensile method was found to range from 25°C to 1000°C.

2. Experimental Procedure

2.1. Sample preparation and characterization

Two different SiC coating layers and soda-lime glass were used in this study. The SiC coatings were deposited onto graphite substrates. A conventional hot-wall, low-pressure chemical vapor deposition (LPCVD) technique was used to deposit the SiC coating layers. MTS (CH CH_3SiCl_3, methyl-trichlorosilane) and a dilution gas (hydrogen) were used as the sources of silicon and carbon, respectively. MTS and H_2 were mixed at a ratio of 5 : 1, and the total flow rate was fixed at 800 sccm. The pressure in the reaction chamber was maintained at 20 Torr, and the deposition time was 1 h. The deposition temperature ranged from 1300°C to 1350°C.

The phase and crystal orientations were characterized by an X-ray diffractometer (XRD, Rigaku, D/MAX-IIIC X-ray diffractometer, Tokyo, Japan) with CuKa radiation (λ = 0.15406 nm at 40 kV and 45 mA). The top surfaces and the microstructures of the SiC coatings under each condition were characterized by scanning electron microscopy (S-4800, Hitachi, Japan) and transmission electron microscopy (FE-TEM Tecnai G2 F30, FEI Company, Netherlands). The top surface was obtained as fabricated and the cross-sectional surface was observed after fracturing. The TEM samples were prepared using a focused ion beam (DB-FIB, Nova200, Netherlands). Samples were characterized by Raman spectroscopy (LabRAM HR UV/Vis/NIR, Horiba Jobin Yvon, France). The Raman analysis was conducted to provide a more comprehensive phase characterization than XRD, which was unable to detect the free Si or C in the SiC coatings.[15)]

2.2. Preparation of the tensile specimens

The SiC coating layer was deposited onto graphite. Fig. 1 shows a schematic diagram of the preparation of the tensile specimens. A laser patterning technique with a nanosecond laser (MicroAblater M2000E/Y) machine was used to create a dog-bone-shaped tensile specimen (Fig. 1(b)). Using the laser writing process, detrimental surface and edge-machining damage can be minimized. As the SiC coating layer has high strength, laser which has a wavelength of 355 nm and power of 4.3 W should be applied five times on the SiC coating layer for complete cutting (Fig. 1(b)). The laser-patterned SiC specimens were heat-treated in a box furnace at 800°C for 3 h at a heating rate of 5 C/min in air to eliminate the graphite substrate. Finally, a laser-patterned free-standing SiC coated layer was obtained from the graphite substrate (Fig. 1(c)). The specimen has a total length of 13

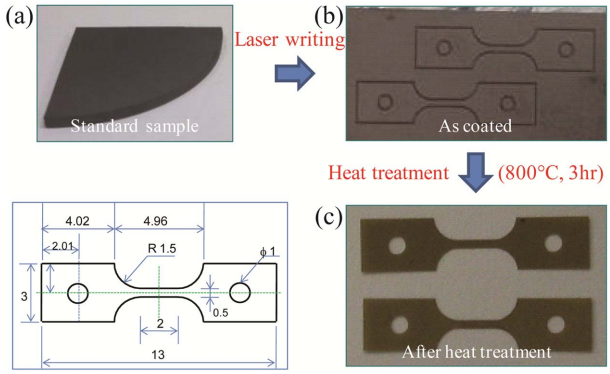

Fig. 1. Schematic diagram of the preparation of the tensile specimen: (a) Standard sample: the SiC coating layer was deposited onto a graphite substrate, (b) laser writing was done on sample with a dog-bone-shaped tensile specimen, and (c) the laser-patterned SiC specimens were heat-treated to separate them from the graphite substrate.

mm and a gauge length of 2 mm. It also had a narrow gauge width of 500 μm. These small and narrow dimensions of the specimen are identical to those of actual TRISO particles.

2.3 High-temperature micro-tensile test

Tensile testing is preferred for structural materials because it creates a uniform state of stress and strain and enables their direct measurement. However, gripping and alignment issues make tensile tests difficult for brittle materials. Various methods for the micro-tensile testing of SiC coatings have been proposed, such as the specimen end inserted in holder, a specimen fixed onto the holder using adhesives, a grip holder to grip a specimen, and a holed specimen loaded on a holder using pins.[16-20)] The present study developed a new grip method by which the specimen was fixed onto small ceramic holders and held by a ceramic pin. A thin and brittle SiC tensile specimen was used for the high-temperature micro-tensile test using an Instron 8848 micro-tester (Micro Force System, Instron, USA). The micro-tensile-test system consists of a static load cell, an Al_2O_3 holder, an Al_2O_3 jig, a Si_3N_4 pin, a clamshell furnace, and a water cooler in consideration of the high-temperature test. Figs. 2(a) and (b) show a schematic diagram of the newly developed micro-tensile-testing system and the fabricated micro-tensile sample for the fracture strength characterization of SiC coatings in the temperature range of 25°C to 1000°C. As the SiC specimen was too thin to handle for the tensile test with the pin-type grip, a ceramic jig was selected in order to support the specimen safely (Fig. 2 (b)). Two ceramic jigs were attached to each other with commercial glue. The adhesive force of commercial glue was loosened at temperatures exceeding 200°C. The Al_2O_3 jig and the specimen were fixed with a ceramic adhesive (Toku Ceramics P-24, Japan) which is stable at high temperatures (< 1300°C).

Soda-lime glass (Menzer, Germany) was used for the con-

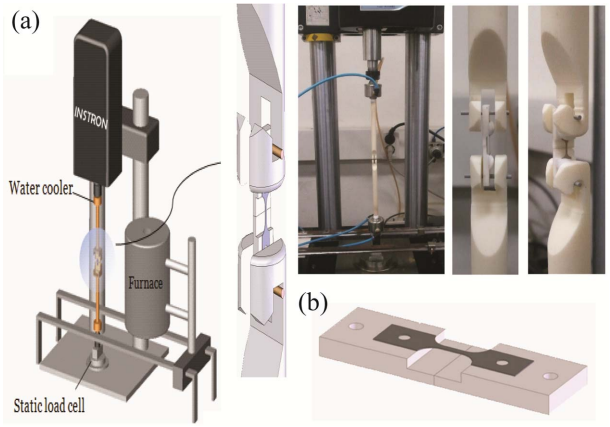

Fig. 2. (a) Schematics of the high-temperature micro-tensile test and the experimental setup, and (b) SiC tensile specimen on the ceramic jig.

firmation and standardization of the newly developed micro-tensile test procedure. The strength value of soda-lime glass is well known, and nature of brittle fractures is similar to the failure characteristics of SiC coatings. The soda-lime glass was cut into 3 mm x 7 mm pieces at a thickness of 150 mm and the flaws on both sides of the edges were removed. Thus, one side of the fabricated soda-lime glass tensile specimens was abraded with 400-grit SiC abrasive powder, which induces uniformly distributed flaws on the surfaces of the glass specimens.

The SiC tensile specimen and soda-lime glasses fixed on either end to Al_2O_3 jigs were loaded onto a ceramic holder using a Si_3N_4 pin and placed inside the furnace, as shown in Fig. 2(a). The furnace heated the specimens to 1000°C at a heating rate of 25 C/min, and they were held at this temperature for 10 min to stabilize the furnace before the test.

In order to protect the specimens from fracturing caused by the heat expansion of the holders, we used the load-protect system of the Instron 8848 micro-tester. This system moves the actuator to maintain the force loaded onto a specimen at ±0.1 N. The actuator moves at a crosshead speed of 10 mm/s until the specimens fail and a load drop occurs.

3. Results and Discussion

3.1. Microstructure

Two different SiC coating layers, which we designate as SiC-A and SiC-B, were used in this study. The SiC coating layer used in this study was primarily highly faulted FCC b-SiC. X-ray diffraction (XRD) patterns of the corresponding SiC coating layers are shown in Fig. 3. The preferred orientation of SiC-A was the (111) direction, while SiC-B had the (220) preferred direction. The microstructures of the two CVD-SiC coating layers also differed (Fig. 4). SiC-A exhibited a thin thickness (~30 mm) and an isotropic and domed shape top surface, while SiC-B had a thick thickness (~50 mm) and a columnar and faceted shape top surface. According to previous studies, the microstructure and preferred

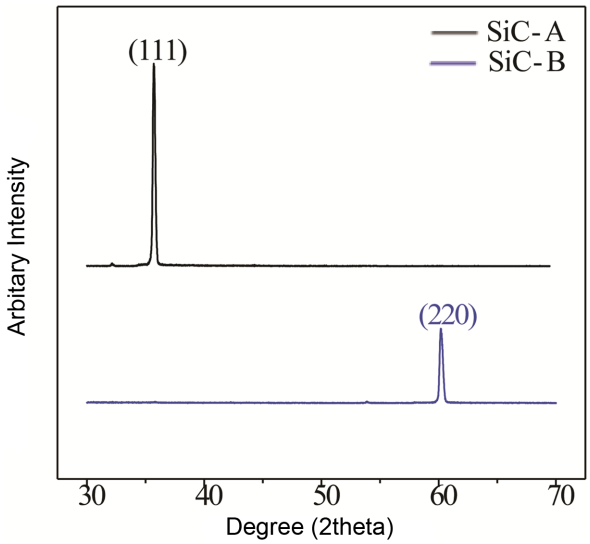

Fig. 3. XRD patterns of two SiC coating layers.

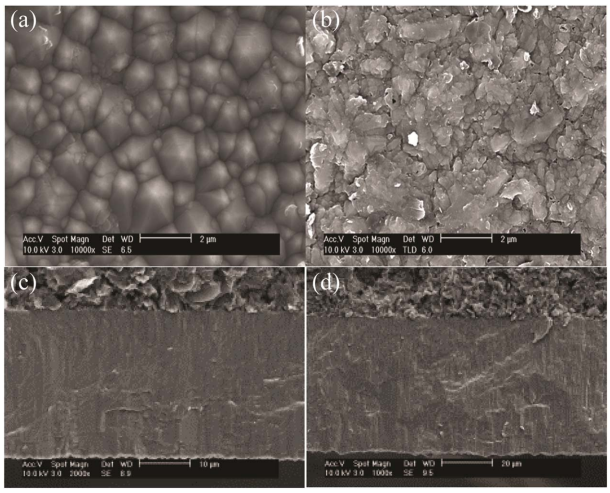

Fig. 4. Microstructure of (a) the surface area, (c) the cross-sectional area of SiC-A, and (b) the surface area, (d) the cross-sectional area of SiC-B.

orientation of CVD-SiC differ depending on the deposition process. Thus, the differences in the microstructures and preferred orientations are due to the deposition mechanism, as reported in the literature.[21,22]

3.2. High-temperature micro-tensile-test

3.2.1. Validation of the developed method using soda-lime glass

Prior to the fracture strength of the SiC coatings, the developed method was validated with standard specimens. To confirm the validation of the developed method, a soda-lime glass with a bending strength of 50~150 MPa and a tensile strength of 25~60 MPa was selected as a standard specimen owing to its brittle fracture behavior.[23-25]

In Figs. 5(a) and (b), the fracture strength and a Weibull diagram of strengths for soda-lime glass specimens as obtained from the proposed test method at room tempera-

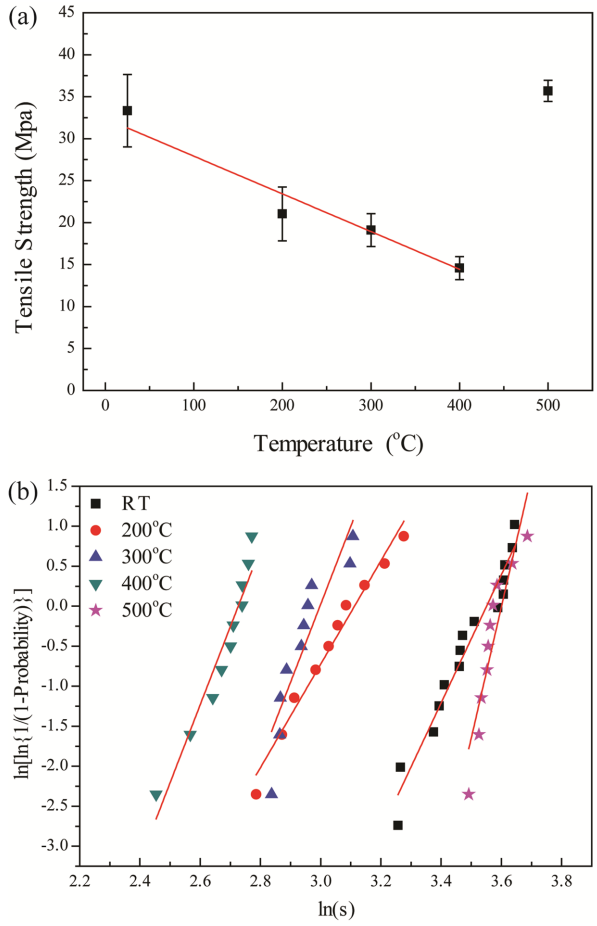

Fig. 5. Micro-tensile test results of soda-lime glass from room temperature to a high temperature: (a) tensile strength, and (b) Weibull modulus.

ture and at a high temperature are shown. In Fig. 5(a), the average tensile strength and range of the observed tensile strength are plotted. The average tensile strength of each sample decreases with an increase in the testing temperature. In order to investigate the testing results closely, Weibull plots of the tensile strength of soda-lime glass are shown in Fig. 5(b). Each plot shows the result of each tensile test. The lines in the plots are fitting lines to the Weibull distribution function, and slope of each line is the Weibull modulus at each test temperature.

A fracture strength of 33.54 MPa and a Weibull modulus of 8.01 at room temperature are typical for soda-lime glass with an artificial flaw on the surface, slightly abraded with 400-grit SiC abrasive powder. According to the Griffith theory, flaw or crack sizes can be considered as being a few micrometers wide. The fractures strength of soda-lime glass decreased as the testing temperature increased below 400°C, but the fracture strength of soda-lime glass measured at 500°C was higher than that at room temperature. The fracture strengths of soda-lime glass at a high temperature decreased because the atomic movement is free at a high temperature. The high fracture strength measured at

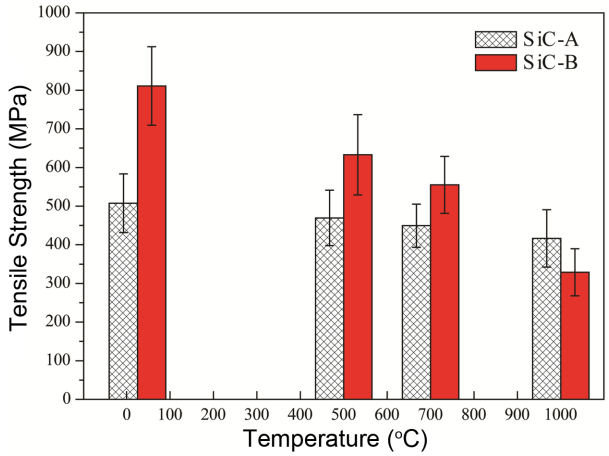

Fig. 6. Tensile strength of two SiC layers at room temperature and at a high temperature.

500°C, which is near the glass transition temperature, appears to have been caused by the crack healing of flaw cracks around the surfaces and edges. In a previous study of the crack healing phenomenon of soda-lime glass, crack healing appears around the glass transition temperature and with an increase in the fracture strength.[26-28] From the results of the soda-lime glass, the developed micro-tensile test was standardized and verified successfully.

3.2.2. Fracture strength of SiC coatings from room temperature (RT) to a high temperature (HT)

In the present study, the newly developed high-temperature micro-tensile test method was applied to compare the strengths of the two SiC coating layers (SiC-A, and SiC-B) measured from 25°C to 1000°C. For each specimen, fifteen tests were conducted at 25°C, and ten were done at 500, 700 and 1000°C. All specimens showed the expected brittle fracturing behavior. Fig. 6 shows the relationship between the fracture strength of the SiC coatings and the test temperatures, and the average facture strength and range of the observed fracture strength are plotted. In order to determine the Weibull modulus, Weibull plots of the tensile strengths of the SiC layers are shown in Figs. 7 (a) and (b). The slope of each line in the plots fitted to the Weibull statistics is the Weibull modulus of each sample and the testing temperature. The results of the fracture strength and the Weibull modulus of the SiC coatings at each temperature are summarized in Table 1.

For SiC-A, the room-temperature fracture strength was 507.53 MPa, the Weibull modulus was 6.68, and the standard deviations were approximately 15% of the average fracture strength. A room temperature fracture strength of 810.82 MPa, a Weibull modulus of 7.99, and standard deviations of about 12% of the average fracture strength were obtained for SiC-B. The fracture strength and Weibull modulus of SiC-B, showed a faceted-columnar microstructure with the preferred orientation on the (220) plane, larger than that of SiC-A, which exhibited a round-stratified

Table 1. Results of the Micro-Tensile-Test

	Temperature (°C)	Fracture strength (MPa)	Standard deviation (MPa)	Weibull Modulus
SiC-A	25	507.53	75.72	6.68
	500	469.43	71.49	6.24
	700	449.37	55.87	7.71
	1000	416.30	74.23	5.53
SiC-B	25	810.82	101.35	7.99
	500	632.81	103.95	5.95
	700	555.14	73.57	6.92
	1000	328.67	60.88	5.05

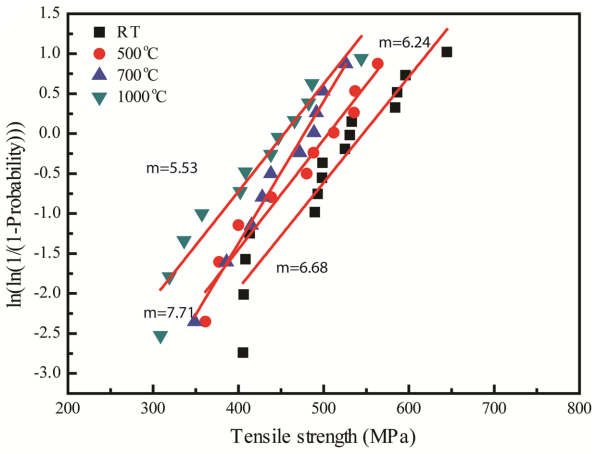

(a) SiC-A

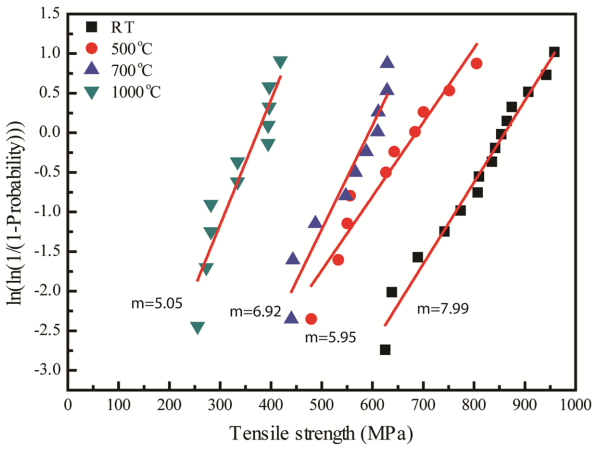

(b) SiC-B

Fig. 7. Weibull modulus of two SiC layers: (a) the SiC-A coating layer, and (b) the SiC-B coating layer at room temperature and at a high temperature.

microstructure with a preferred orientation on the (111) plane. The difference in the fracture strength and Weibull modulus value of each specimen may be due to the microstructure and crystal orientation of the coatings.[29,30] In an early study concerning the failure probability of TRISO nuclear fuel particles, the Weibull modulus was found to be an important factor in reducing the failure probability of TRISO nuclear fuel particles.[31] A high Weibull modulus value is necessary for a safer design of TRISO nuclear fuel particles.

As the test temperature increased, the fracture strength of the SiC coatings decreased. For SiC-A, fracture strengths of 469.43, 449.37, and 416.30 MPa were measured at 500, 700, 1000°C, respectively. Also, Weibull moduli of 6.24, 7.71, and 5.53 were measured correspondingly at 500, 700, and 1000°C. In contrast, for SiC-B, fracture strengths of 632.81, 555.14, and 328.67 MPa and Weibull moduli of 5.95, 6.92, and 5.05 were measured at 500, 700 and 1000°C, respectively. The two different SiC coating layers showed different fracture behavior at elevated temperatures. Although SiC-B had higher fracture strength at room temperature than SiC-A, the strength of SiC-B at 1000°C became lower than that of SiC-A. This phenomenon may have been caused by the internal microstructural differences between two SiC layers.

3.3. Internal structure analysis

The high-resolution transmission electron microscopy (HRTEM) examination indicates the existence of an internal structure with close-packed defects. Fig. 8 shows HRTEM images of SiC-A and SiC-B. According to the HRTEM images, SiC-A and SiC-B have different internal structures. SiC-A has a larger columnar grain boundary than SiC-B and the columnar grain boundary of SiC-A is clean. On the other hand, SiC-B has a small columnar grain size with defects inside. Fig. 8(d) shows that the other phase was located along the grain boundary and that stacking fault defects existed in the grain of SiC-B. SiC-B had higher fracture strength than SiC-A according to the room-temperature test. In terms of the grain-size, SiC-B had a naturally higher strength than SiC-A because smaller grain sizes are generally related to higher strength materials and less diffusion of the fission products. The result of the micro-tensile-test at room temperature was in good agreement with TEM analysis results (Fig. 8).

The SiC-B coating layer also had another phase along the grain boundary. Thus, we identified the other phase from the diffraction pattern with HRTEM (Fig. 9). Four different areas were selected and the diffraction patterns were con-

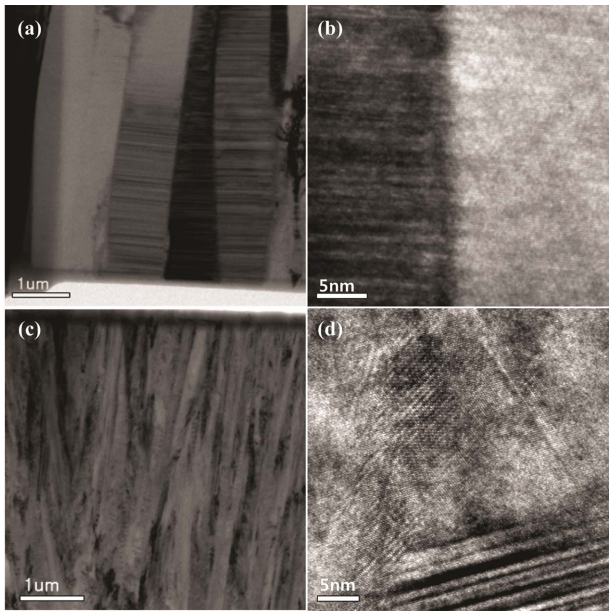

Fig. 8. TEM images of (a) and (b), SiC-A and (c) and (d), SiC-B.

firmed for each. With these diffraction patterns, regions 2, 3, and 4 was identified as having only the beta-SiC phase. On the other hand, region 1 showed a beta-SiC pattern outside and a residual silicon pattern inside. Residual Si was located along the grain boundary in the SiC-B coating layer.

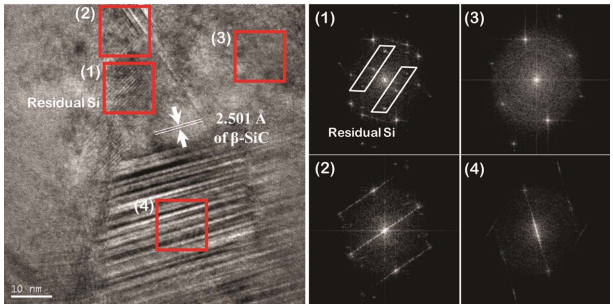

Fig. 9. HRTEM of SiC-B and electron diffraction pattern of four different areas of SiC-B. Regions (2, 3, 4) were identified as the beta-SiC phase. On the other hand, region (1) showed beta-SiC patterns on the outside and residual silicon patterns inside (white parallelogram).

To characterize the presence of free Si, a Raman analysis was conducted. Fig. 10 shows the Raman shift of the SiC coating layers. From these plots, broad TO (zone-center transverse optical phonon mode) and LO (zone-center longitudinal phonon mode) signals in the region of 650 to 1050 cm^{-1} are shown. For two samples, an additional band at 1500 cm^{-1} was identified as a second-order band of SiC.[15] In previous work, at temperatures below at 1500°C, Si was co-deposited due to the low surface reactivity of the carbon species participating in the formation of SiC.[15,32,33]

Residual Si was found to exist only in SiC-B according to the Raman spectroscopy analysis results and the results of

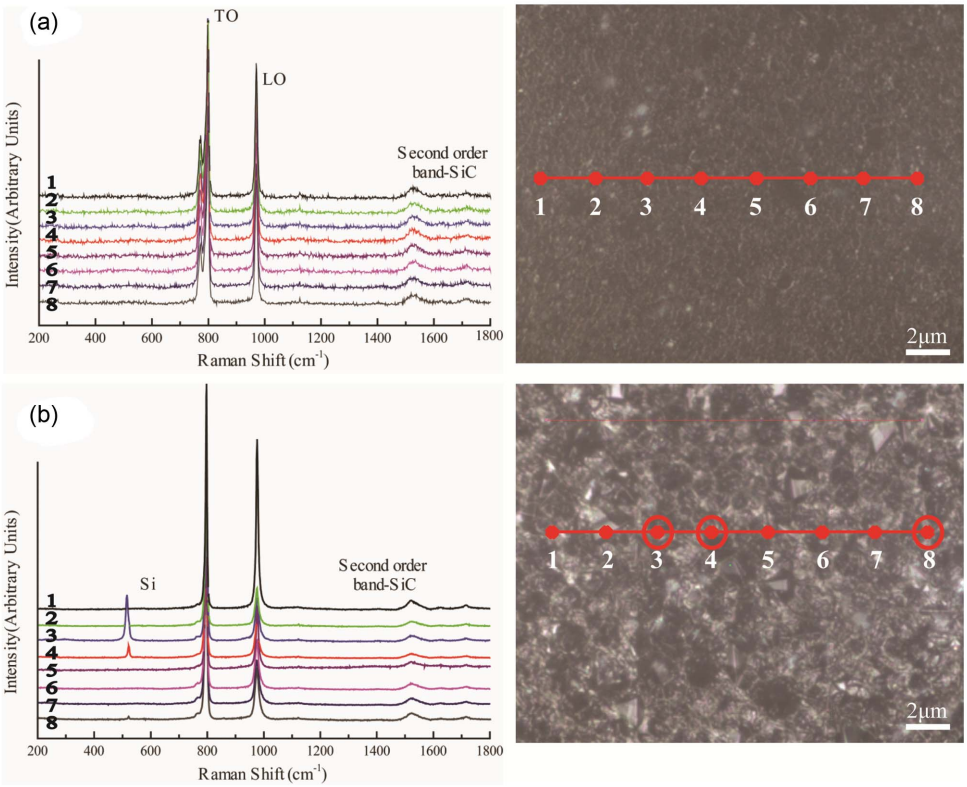

Fig. 10. Raman spectroscopy of (a) SiC-A and (b) SiC-B.

a TEM internal structural analysis. This difference in the microstructure causes different fracture behaviors at elevated temperatures. The SiC coatings produced below 1500°C had free Si due to the low surface reactivity of the carbon species participating in the formation of SiC, and it appear that the presence of free Si seriously degrades the fracture strength and limits the use of this material at elevated temperatures.[33,34] The degradation of the strength was attributed to misfit strains between the SiC and free Si phases causing the critical flaws to increase in size.[32] The presence of free Si in TRISO fuel particles SiC is known,[35] though its importance not fully recognized.

The fracture strength of SiC-B significantly decreased, while that of SiC-A maintained its strength from RT to HT. The decrement of the temperature-dependent fracture strength was also related to the microstructure and defects of the SiC coatings. In these results, SiC-A showed a larger columnar grain size, no free Si, no stacking faults, a small decrement of the fracture strength and a large Weibull modulus at high temperatures, all acceptable criteria to create mechanically reliable TRISO nuclear fuel particles which can be used at high temperatures.

4. Conclusions

SiC coatings for TRISO nuclear fuel particles were fabricated by a chemical vapor deposition method. For the characterization of the high-temperature fracture strength of the SiC coatings, a high-temperature micro-tensile-method was newly developed and the fracture strengths were measured by the micro-tensile method up to 1000°C. Two different types of SiC layers were prepared, termed SiC-A and SiC-B in this study. SiC-A exhibited a larger columnar grain size (0.4 ~ 0.6 mm), a round top surface, and the [111] preferred orientation, while SiC-B had a small columnar grain size (0.2 ~ 0.3 mm), a faceted top surface, and the [220] preferred orientation. The fracture strengths of the SiC coatings, as measured by the high-temperature micro-tensile test, decreased at an elevated temperature. The fracture strength decrement of SiC-A was smaller than that of SiC-B. The high-temperature mechanical properties of the SiC coatings were related to the microstructure and defects, and SiC-A showed high stability and reliability levels at a high temperature. From the results, it can be concluded that SiC-A is a good coating candidate for the safe design of TRISO nuclear fuel particles operating at high temperatures.

REFERENCES

1. A. G. Evans, D. R. Mumm, J. W. Hutchinson, G. H. Meier, and F. S. Pettit, "Mechanisms Controlling the Durability of Thermal Barrier Coatings," *Prog. Mater. Sci.*, **46** 505-53 (2001).
2. S. G. Hong, T. S. Byun, R. A. Lowden, L. L Snead, and Y. Katoh, "Evaluation of the Fracture Strength for Silicon Carbide Layers in the Tri-Isotropic-Coated Fuel Particle," *J. Am. Ceram. Soc.*, **90** 184-91 (2007).
3. R. Scholz, "Deuteron Irradiation Creep of Chemically Vapor Deposited Silicon Carbide Fibers," *J. Nucl. Mater.*, **254** 74-7 (1998).
4. C. H. Tang, Y. P. Tang, J. G. Zhu, Y. W. Zou, J. H. Li, and X. J. Ni, "Design and Manufacture of the Fuel Element for the 10 MW High Temperature Gas-Cooled Reactor," *Nucl. Eng. Des.,* 91-102 (2002).
5. S. Nakao, T. A, K. Sato, "Mechanical Characterization of SiC Film at High Temperatures by Tensile Test," IEEE, MEMS 2008, Tucson, AZ, USA, January 13-17, 2008.
6. W.N. Sharpe, O. Jadaan, G. M. Beheim, G. D. Quinn, and N. N Nemeth, "Fracture Strength of Silicon Carbide Micro Specimens," *J. Microelectromech. Syst.*, **14** 903-13 (2005).
7. T. D. Gulden, C. L. Smith, and D. P Harmon, "Mechanical Design of TRISO-Coated Particle Fuels for the Large HTGR," *Nucl. Technol.*, **16** 100-9 (1972).
8. H. Nabielek, W. Kuhnlein, and W. Schenk, "Development of Advanced HTR Fuel Elements," *Nucl. Eng. Des.*, **121** 199-210 (1990).
9. B. G. Kim, Y. Choi, J. W. Lee, Y. W. Lee, D. S. Sohn, and G. M. Kim, "Multi-Layer Coating of Silicon Carbide and Pyrolytic Carbon on UO_2 Pellets by a Combustion Reaction," *J. Nucl. Mater.,* **281** 163-70 (2000).
10. G. K. Miller, D. A. Petti, D. J. Varacalle, and J. T. Maki, "Statistical Approach and Benchmarking for Modeling of Multi-Dimensional Behavior in TRISO-Coated Fuel Particles," *J. Nucl. Mater.,* **317** 69-82 (2003).
11. K. Minato and K. Fukuda, "Chemical Vapor Deposition of Silicon Carbide for Coated Fuel Particles," *J. Nucl. Mater.,* **149** 233-46 (1987).
12. H. Nickel, H. Nabielek, G. Pott, and A.W. Mehner, "Long Time Experience with the Development of HTR Fuel Elements in Germany," *Nucl. Eng. Des.*, **217** 141-51 (2002).
13. S. J Xu, J. G. Zhou, B. Yang, and B. Z. Zhang, "Effect of Deposition Temperature on the Properties of Pyrolytic SiC," *J. Nucl. Mater.,* **224** 12-6 (1995).
14. J. H. Kim, H. K. Lee, and D. K. Kim, "Strength Measurement of a Brittle Coating with a Trilayer Structure Using Instrumented Indentation and in situ Observation Techniques," *Philos. Mag.,* **86** 5383-96 (2006).
15. E. H. Lopez, P. J. Meadows, J. Tan, and P. Xiao, "Control of Stoichiometry, Microstructure, and Mechanical Properties in SiC Coatings Produced by Fluidized Bed Chemical Vapor Deposition," *J. Mater. Res.,* **23** 1785-96 (2008).
16. M. T. Lin, P. El-Deiry, R. R. Chromik, N. Barbosa, W. L. Brown, T. J. Delph, and R. P Vinci, "Temperature-Dependent Microtensile Testing of Thin Film Materials for Application to Microelectromechanical System," *Microsyst. Technol.,* **12** 1045-51 (2006).
17. R. Liu, H. Wang, X. P Li, G. F. Ding, and C. S. Yang, "A Micro-tensile Method for Measuring Mechanical Properties of MEMS Materials," *J. Micromech. Microeng.*, **18** 65002-7 (2008).
18. R. Modlinski, R. Puers, and I. D. Wolf, "AlCuMgMn Micro-Tensile Samples - Mechanical Characterization of MEMS Materials at Micro-Scale," *Sens. Actuators. A. Phys.*, **143** 120-28 (2008).

19. J. H. Park, M. S. Myung, and Y. J. Kim, "Tensile and High Cycle Fatigue Test of Al-3% Ti Thin Films," *Sens. Actuators. A. Phys.*, **147** 561-69 (2008).
20. W. N. Sharpe, G. M. Beheim, L. J. Evans, N. N. Nemeth, and O. M. Jadaan, "Fracture Strength of Single-Crystal Silicon Carbide Microspecimens at 24 Degrees C and 1000 Degrees C," *J. Microelectromech. Syst.*, **17** 244-54 (2008).
21. D. J. Kim, D. J. Choi, Y. W. Kim, "Effect of Reactant Depletion on the Microstructure and Preferred Orientation of Polycrystalline Sic Films by Chemical-Vapor-Deposition," *Thin Solid Films*, **266** 192-97 (1995).
22. H. S. Kim and D. J. Choi, "The Reactant Depletion Effect on Chemically Vapor Deposited SiC Films with Pressure and Gas Ambient," *Thin Solid Films*, **312** 195-201 (1998).
23. Soda-lime glass. Data sheet, CiDRA Precision Services;LLC.
24. Soda-lime glass. Data sheet, Metroglasstech.
25. Soda-lime glass. Data sheet, Fa. Technolgas.
26. M. K. C. Holden and V. D. Frechette, "Healing of Glass in Humid Environments," *J. Am. Ceram. Soc.*, **72** 2189-93(1989).
27. T. E. Wilantewicz and J. R. Varner, "Vickers Indentation Behavior of Several Commercial Glasses at High Temperatures," *J. Mater. Sci.*, **43** 281-98 (2008).
28. B. A. Wilson and E. D. Case, "In situ Microscopy of Crack Healing in Borosilicate Glass," *J. Mater. Sci.*, **32** 3163-75 (1997).
29. A. Elkind and M. W. Barsoum, "Grain Growth and Strength Degradation of SiC Monofilaments at High Temperatures," *J. Mater. Sci.*, **31** 6119-23 (1996).
30. H. Zhang, J. Tian, W. Tang, and F. Lu, "Correlation between Fracture Strength and Crystal Orientation of Freestanding Diamond Films," *Carbon*, **41** 579-625 (2003).
31. B. Liu, T. X. Hang, and C. H. Tang, "A Review of TRISO-coated Particle Nuclear Fuel Performance Models," *Rare Metals*, **25** 337-42 (2006).
32. R. J. Price and G. R. Hopkins, "Flexural Strength of Proof-Tested and Neutron-Irradiated Silicon Carbide," *J. Nucl. Mater.*, **108 & 109** 732-38 (1982).
33. B. O. Yavuz and R. E. Tressler, "High Temperature Mechanical Behavior of a Chemically Vapor Deposited Beta Silicon Carbide," *Ceram. Int.,* **18** 19-26 (1992).
34. A. Briggs, R. W. Davidge, C. Padgett, and S. Quickenden, "Crushing Behavior of High Temperature Reactor Coated Fuel Particles," *J. Nucl. Mater.*, **61** 233-42 (1976).
35. A. Naoumidis, R. Benz, and J. Rottman, "Identification of Silicon in Small Quantities of SiC-Coated and SiC (TRISO)-Coated Nuclear Fuel Particles," *High. Temp. High. Press.*, **14** 53-63 (1982).